Protein Adsorption

DOI: 10.1002/anie.201406349

# Reversibly Controlling Preferential Protein Adsorption on Bone Implants by Using an Applied Weak Potential as a Switch**

*Jingwen Liao, Ye Zhu, Zhengnan Zhou, Junqi Chen, Guoxin Tan,* Chengyun Ning,* and Chuanbin Mao**

***Abstract:*** *A facile method is needed to control the protein adsorption onto biomaterials, such as, bone implants. Herein we doped taurocholic acid (TCA), an amphiphilic biomolecule, into an array of 1D nano-architectured polypyrrole (NAPPy) on the implants. Doping TCA enabled the implant surface to show reversible wettability between 152° (superhydrophobic, switch-on state) and 55° (hydrophilic, switch-off state) in response to periodically switching two weak electrical potentials (+0.50 and −0.80 V as a switch-on and switch-off potential, respectively). The potential-switchable reversible wettability, arising from the potential-tunable orientation of the hydrophobic and hydrophilic face of TCA, led to potential-switchable preferential adsorption of proteins as well as cell adhesion and spreading. This potential-switchable strategy may open up a new avenue to control the biological activities on the implant surface.*

The clinical success of orthopedic and dental implants, represented by biomedical titanium, heavily relies on the osteointegration at the interface between the implants and host tissue.[1] The optimal osteointegration, without fibrous tissue growth at the interface, stems from the optimal characteristics of the implant surface in close proximity with the bone tissue.[2] The surface characteristics of the implants, in particular the wettability, in conjunction with the host's cells, determine the biological responses at the implant surface.[3] The protein adsorption on the implants is the first biological response. It is often dependent on the wettability, which is determined by surface chemistry and topography.[4d,5,6] It tends to develop a "conditioning film" for modulating the host's cellular response, such as the adhesion, spreading, proliferation, and differentiation, and consequently, bonic tissue growth on the implants.[4] Most implant materials have non-variable surface wettability. Therefore, tuning their surface wettability has been proposed to control their biological activities.[2b,4d,7] Ideally, an implant should be "intelligent" so that it is able to reversibly adsorb different proteins through reversible wettability. For instance, a protein that can be secreted by cells and promote cell adhesion and spreading, such as fibronectin (Fn),[8] can be selectively adsorbed onto the implant at the early stage of the implantation; a growth factor, such as bone morphogenetic protein-2 (BMP-2),[9] that can promote osteogenesis and osteointegration can be selectively adsorbed onto the implant at the late stage of implantation. However, simply manipulating the surface chemistry and roughness cannot achieve a reversible switch of surface wettability. Herein we demonstrate the first-time use of a conducting polymer, polypyrrole (PPy), doped with a biomolecule, taurocholic acid (TCA), which can be found in bile and biosynthesized from cholesterol in the liver,[10] to achieve the reversible switch of surface wettability (Scheme 1) and the subsequent reversible protein adsorption as well as cell adhesion and spreading on the implants in response to a weak potential switch.

PPy is a class of functional polymers with electroactivity derived from their molecular structures[11] and a promising biomaterial owing to its excellent tissue compatibility.[12] A dopant is needed to control its properties.[13] However, the perfluorinated dopant (for example, perfluorooctanesulfonic acid) currently being used in PPy is not suitable for biomedical use as it is an organic pollutant.[14] Hence, from the perspective of biomedical applications, there is a pressing need in a new approach to tuning the properties, such as wettability, through the use of non-toxic molecules.[15]

Herein we propose TCA as such a non-toxic molecule. It has special pharmaceutical effects, such as anti-inflammation

[*] J. Liao,[+] Z. Zhou, J. Chen, Prof. C. Ning
School of Materials Science and Engineering
South China University of Technology
Guangzhou 510641 (China)
E-mail: imcyning@scut.edu.cn
Y. Zhu,[+] Prof. C. Mao
Department of Chemistry & Biochemistry
Stephenson Life Sciences Research Center
University of Oklahoma (USA)
E-mail: cbmao@ou.edu
G. Tan
Institute of Chemical Engineering and Light Industry
Guangdong University of Technology
Guangzhou 510006 (China)
E-mail: tanguoxin@126.com
[+] These authors contributed equally to this work.

[**] This work was supported by the National Basic Research Program of China (Grant No. 2012CB619100) and the National Natural Science Foundation of China (Grant Nos. 51372087, 51072057). Y.Z. and C.M. would like to thank the financial support from National Institutes of Health (EB015190), National Science Foundation (CBET-0854414, CMMI-1234957, and DMR-0847758), Department of Defense Peer Reviewed Medical Research Program (W81XWH-12-1-0384), Oklahoma Center for Adult Stem Cell Research (434003), and Oklahoma Center for the Advancement of Science and Technology (HR14-160). We would like to thank Xuliang Deng's group at Peking University for their assistance during the experiments.

Supporting information (experimental details) for this article is available on the WWW under http://dx.doi.org/10.1002/anie.201406349.

  

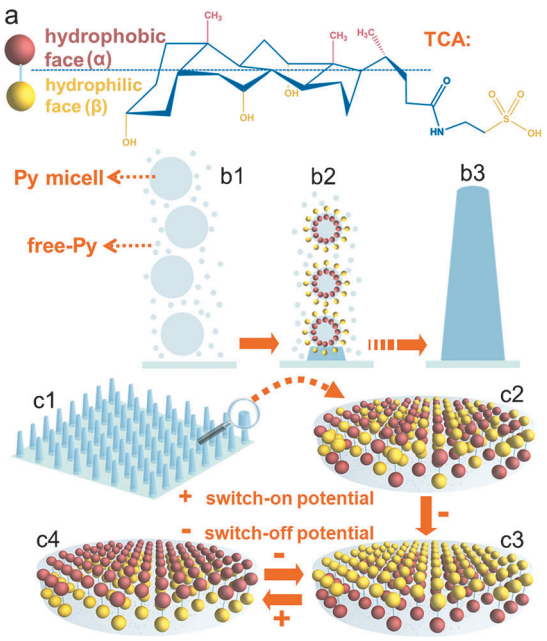


***Scheme 1.*** a) The chair conformation of TCA. b) The possible mechanism of forming 1D NAPPy/TCA (b3) through the self-assembly and polymerization of Py droplets and free-Py (see text for details). c) Proposed mechanism of the electrical-potential-switchable wettability of 1D NAPPy/TCA: c1–c2) The orientation of hydrophobic α-face and hydrophilic β-face of TCA was random in the absence of an applied potential. c3) The hydrophilic β-face of TCA was exposed on the surface of the implants when a switch-off potential was applied to the implants. This state was termed as switch-off. c4) When a switch-on potential was applied, the hydrophobic α-face is exposed on the surface, making the implant surface more hydrophobic. This state was termed as switch-on.

and cough relief. The chair conformation of TCA (Scheme 1a) indicates a unique facial amphiphilicity. Namely, it bears a distinguishable hydrophobic face (α-face) and hydrophilic face (β-face)[16] owing to the exposure of -$CH_3$ and -OH/-$SO_3$H groups, respectively. Herein TCA was employed as a surfactant-like dopant molecule to guide the self-assembly and polymerization of pyrrole (Py) nanodroplets (i.e., Py micelles) along with free-Py into conical 1D nano-architectured polypyrrole (NAPPy) (Scheme 1b1–b3) on the biomedical titanium implants. The TCA molecule was expected to change the orientation of its α-face and β-face in the PPy matrix in response to periodic switching of potentials (Scheme 1c). We found that an appropriate concentration of TCA was indispensable in the fabrication of 1D NAPPy on the titanium. Moreover, the electrical-potential-induced molecular orientation switch between the α-face and β-face of TCA was used to achieve electrical-potential-induced surface wettability of the 1D NAPPy/TCA. To demonstrate the possible use of the potential-induced wettability and thus the response of the conducting polymers on biomedical titanium, we showed that the potential-induced wettability led to the preferential adsorption of three model proteins (Fn, bovine serum albumin (BSA), and protamine sulfate (PAS)) as well as controlled adhesion and spreading of MC3T3-E1 osteoblasts on 1D NAPPy/TCA.

In an attempt to study the effect of TCA as a biosurfactant on the fabrication of NAPPy/TCA through template-free electrochemical polymerization, it was found that the nano-architectures of PPy were dependent on the concentration of TCA in PBS. When the concentration of TCA was increased from 0.01 M to 0.07 M, and finally to 0.20 M, the PPy evolved from irregular films (Figure 1a) to 1D

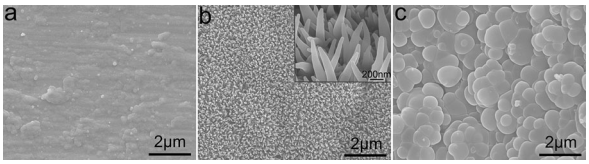


***Figure 1.*** Field emission scanning electron microscopy (FE-SEM) images of NAPPy/TCA obtained in PBS containing 0.01 M (a), 0.07 M (b), and 0.20 M (c) of TCA. Inset in (b): higher magnification.

conical nanowires (Figure 1b), and to tightly packed microparticles (Figure 1c). We believe that it is important for anionic dopants, such as TCA, to act like surfactants to stabilize the dispersion of Py nanodroplets in PBS (as the electrolyte). The Py nanodroplets self-assembled into column-like 1D structures and polymerized to form 1D NAPPy (Scheme 1b). When a lower concentration of TCA (0.01 M) was used, not enough TCA was captured by the Py nanodroplets, the nanodroplets were not sufficiently stabilized by TCA and thus failed to self-assemble along one direction into columns. Consequently, an irregular film (Figure 1a) was obtained by the polymerization of the nanodroplets and dissolved free Py. When the TCA concentration was very high (0.2 M), exceeding its critical micelle concentration, TCA formed microscale micelles, which contained dissolved free Py and even Py nanodroplets. As a result, tightly packed microparticles were obtained (Figure 1c). Py nanodroplets could self-assemble along the direction perpendicular to the substrates to from ordered 1D nano-architectures (Scheme 1b) only if TCA was in an appropriate concentration (0.07 M). In addition, the growth of 1D nano-architectures started from the surface of the substrates. During its elongation, the dissolved free Py monomers were simultaneously polymerized on its outer surface, allowing them to grow along the lateral direction to increase its diameter and consequently leading to the formation of conical nanowires oriented nearly vertically on the substrates (Figure 1b). We studied the adhesion of MC3T3-E1 osteoblasts on the three different PPy/TCA structures as well as on the uncoated Ti substrates. We found that 1D NAPPy/TCA could promote the adhesion when compared to the irregular PPy/TCA films and showed similar capability in promoting cell adhesion as un-coated and PPy/TCA microparticle-coated substrates (Supporting Information, Figure S1). Furthermore, we found that doping TCA in PPy increased the biocompatibility of the 1D NAPPy/TCA (Figure S2).

We then tested the reversible switch in the wettability of 1D NAPPy/TCA by applying periodic potentials of −0.80 V (as a switch-off potential) and +0.50 V (as a switch-on potential) to generate the reduction state (switch-off state)

  

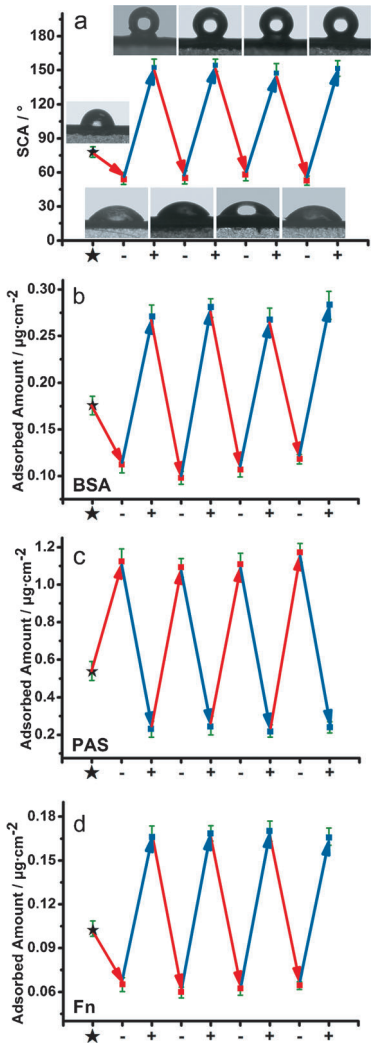


***Figure 2.*** a) The plots of static contact angle (SCA) of 1D NAPPy/TCA and b)–d) plots of the amount of adsorbed BSA (b), PAS (c), and Fn (d) on 1D NAPPy/TCA versus switch-off potentials (−0.80 V) and switch-on potentials (+0.50 V) in situ. Inset in (a): SCA images.

and oxidation state (switch-on state) of 1D NAPPy/TCA, respectively. A reversible switch in wettability (about 152° in switch-on state and 55° in switch-off state) was achieved (Figure 2a). When the dopant was changed to $Cl^-$, the wettability of the doped 1D NAPPy did not switch in response to the change in potential as significantly as for 1D NAPPy/TCA (Figure S3), suggesting the unique role of the TCA dopant. In addition, the cell viability on 1D NAPPy/TCA after applying periodic switching potentials with different magnitudes showed that the weak potentials (−0.80 V/+0.50 V) we used did not kill osteoblasts (Figure S4).

Through 500 cycles of periodic potential switches, both static contact angle (SCA) in switch-on and switch-off states remained relatively stable (Figure S5). Moreover, the wettability of the switch-on and switch-off states after immersion in physiological medium was nearly unchanged (Figure S6). The TCA was not released from 1D NAPPy/TCA in physiological medium (Figure S7). These data showed that 1D NAPPy/TCA was very stable.

Electron probe micro-analysis (EPMA) (Figure S8a) identified no significant difference in TCA concentration between the two switching states. However, attenuated total reflection Fourier-transform infrared spectroscopy (ATR-FTIR) of specimens in different states (Figure S8b) showed that not only the peaks resulting from -OH/-$SO_3H$ groups on the β-face of TCA were blue-shifted in the switch-off state compared to other states, but also the reduction potential used to generate the switch-off state caused partial deprotonation of -C-OH (on the β-face) to form -C-$O^-$. Furthermore, Kelvin probe force microscopy (KFM) showed that the surface potential (Figure S8c) of the specimen in the switch-off state had a stronger strength of negative charge arising from the polar groups on the β-face of TCA whereas a negligible strength of negative charge was present in the switch-on state. In addition, the surface potential distribution of 1D NAPPy/TCA in the switch-off and switch-on states was greater than that in the original state (Figure S8c), suggesting that the orientation of TCA was uniform (i.e., mainly either α-face or β-face is exposed) across the surface of the 1D NAPPy/TCA under the switching potentials. Together these results indicated the expected change in the orientation of TCA during potential switching (Scheme 1).

We propose a model to understand the potential-induced reversible switch in the wettability of 1D NAPPy/TCA (Scheme 1c). In the original state (Scheme 1c2), TCA with α-face and β-face randomly oriented was uniformly incorporated into the PPy matrix, resulting in a SCA of approximately 78°. Unlike common small molecules, TCA has a unique and large spatial structure (Scheme 1a). Thus TCA would not move out of the PPy matrix but could change its orientation during potential switching. Under a switch-off potential (Scheme 1c3), the PPy matrix became negative, repelling and thus forcing the -OH/-$SO_3H$ polar groups on the β-faces to be exposed on the surface of PPy matrix and consequently generating a hydrophilic surface. It was noteworthy that polar groups, such as -OH and -$SO_3H$, formed intermolecular hydrogen bond, and deprotonation of -OH occurred under the switch-off potential as well, which could be shown by the blue-shifts of the three peaks associated with the -OH/-$SO_3H$ groups and the presence of the C-$O^-$ peak at 905 $cm^{-1}$ in switch-off states (Figure S8b2), respectively. When a switch-on potential was applied (Scheme 1c4), the PPy matrix became positive, thus attracting the polar groups on the β-face of TCA to turn toward the titanium substrate while driving the α-faces of TCA to be uniformly turned toward the PPy surface. Consequently, quite a few of α-faces instead of β-faces were exposed on the PPy surface, making 1D NAPPy/TCA exhibit a superhydrophobic surface. As such, potential-induced reversible switching of wettability (Figure 2a) was in fact a cycle between the states shown in Scheme 1c3 (switch-off state) and Scheme 1c4 (switch-on state). The surface potential characterized by KFM hardly changed for the switch-on and switch-off states before (Figure S8c) and after (Figure S9) MC3T3-E1 osteoblasts were cultured on the 1D NAPPy/TCA, suggesting that cell growth did not alter the orientation of TCA.

Herein, BSA and PAS with an isoelectric point (pI) of about 4.8 and 12.0, respectively, were chosen as model

proteins to test the potential-switchable protein adsorption. It was found that the potential-switchable wettability could be used to control the adsorption of BSA and PAS (Figure 2b and c). The amount of adsorbed protein was monitored by bicinchoninic acid (BCA) assay.[17] Both proteins were reversibly adsorbed on the 1D NAPPy/TCA in response to the changing potentials. However, the two proteins show inverse adsorption profiles (Figure 2b,c). The pI values of BSA and PAS suggested that BSA and PAS were negatively and positively charged at pH 7.4, respectively. The α-faces and β-faces of TCA were exposed on the surface of 1D NAPPy in switch-on and switch-off states, respectively. Therefore, it is difficult for BSA to be adsorbed at pH 7.4 on 1D NAPPy/TCA in the hydrophilic switch-off state owing to repellence by the polar groups (-OH/-$SO_3H$) of β-faces, whereas in the hydrophobic switch-on state more BSA molecules could be adsorbed because of the significantly reduced repellence. Conversely, PAS at pH 7.4 could be adsorbed on 1D NAPPy/TCA in the hydrophilic switch-off state as a result of their attraction to the -OH/-$SO_3H$ of β-faces, while fewer PAS molecules could be adsorbed in hydrophobic switch-on state as a result of greatly reduced attraction. In this way, a reversible switch in preferential protein adsorption can be realized by the potential-induced switch in wettability, which is expected to modulate the biological response on the implant surface in real time. Our work indicates that it is possible to control which protein will preferentially adsorb onto the implants, which in turn will control which biological activity will be activated. As such, a functional adhesion protein, Fn (pI = 5.5), was employed to validate the feasibility of achieving periodically reversible adsorption by a potential-induced switch in wettability. Indeed, Fn showed a similar adsorption profile to BSA because their pI values were very close (Figure 2d).

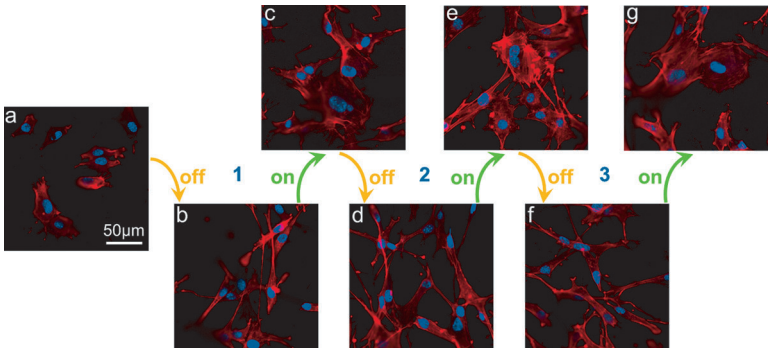


***Figure 3.*** Immunofluorescence staining images of MC3T3-E1 osteoblasts after being seeded on 1D NAPPy/TCA in the original state (a), and cycling between switch-off states (b, d, and f) and switch-on states (c, e, and g) for 8 h: red = F-actin, blue = cell nuclei.

Cells, such as osteoblasts, will secrete Fn and deposit it on the bone implants in bone repair,[8a] which can in turn promote cell adhesion and cell spreading on the implants.[8b,18] Ideally osteoblasts are expected to adhere to and spread on the implants.[3b,19] Hence, we hypothesized that the potential-induced reversible adsorption of Fn secreted by osteoblasts (Figure 2d) could lead to potential-induced reversible adhesion and spreading of osteoblasts on the 1D NAPPy/TCA. To test this hypothesis, MC3T3-E1 osteoblasts were cultured on the 1D NAPPy/TCA during periodic switch-off and switch-on states and their adhesion and spreading were monitored by immunofluorescence imaging. As expected, the potential-induced reversible Fn adsorption onto the 1D NAPPy/TCA (Figure 2d) indeed resulted in reversible cell adhesion (Figure S10) and spreading (Figure 3 and S11), probably because Fn secreted by osteoblasts was preferentially adsorbed onto or desorbed from the 1D NAPPy/TCA in the switch-on or switch-off states, respectively.

In summary, to form "intelligent" implant surfaces that can potentially govern the interfacial biological response in real time, 1D NAPPy was prepared by doping with TCA. The resultant coating displayed a reversible switch in wettability by applying cell-safe, periodic, weak electrical potentials in situ; its switch-on and switch-off states exhibited static contact angles of 152° and 55°, respectively, which was due to the switching of the orientation between α-face and β-face of TCA on the PPy surface. Moreover, such switchable wettability resulted in a reversible switch in the adsorption of various proteins, as well as in the adhesion and spreading of osteoblasts. The facile potential-switchable wettability and protein adsorption will enable us to manipulate the biological response on the implant surface in real time as needed at different implantation stages. Such a potential-induced switch in surface chemistry may also be achieved in other conducting polymers, opening up a new avenue to electrical-potential-responsive intelligent materials.

Received: June 18, 2014
Published online: October 3, 2014

**Keywords:** bone implants · conducting polymers · polypyrroles · protein adsorption · wettability

[1] T. Albrektsson, P.-I. Brånemark, H.-A. Hansson, J. Lindström, *Acta Orthop.* **1981**, *52*, 155.
[2] a) F. Variola, F. Vetrone, L. Richert, P. Jedrzejowski, J. H. Yi, S. Zalzal, S. Clair, A. Sarkissian, D. F. Perepichka, J. D. Wuest, *Small* **2009**, *5*, 996; b) M. Padial-Molina, P. Galindo-Moreno, J. E. Fernández-Barbero, F. O'Valle, A. B. Jódar-Reyes, J. L. Ortega-Vinuesa, P. J. Ramón-Torregrosa, *Acta Biomater.* **2011**, *7*, 771.
[3] a) V. Divya Rani, L. Vinoth-Kumar, V. Anitha, K. Manzoor, M. Deepthy, V. N. Shantikumar, *Acta Biomater.* **2012**, *8*, 1976; b) M. Geetha, A. Singh, R. Asokamani, A. Gogia, *Prog. Mater. Sci.* **2009**, *54*, 397.
[4] a) S.-H. Jun, E.-J. Lee, S.-W. Yook, H.-E. Kim, H.-W. Kim, Y.-H. Koh, *Acta Biomater.* **2010**, *6*, 302; b) S. Okada, H. Ito, A. Nagai, J. Komotori, H. Imai, *Acta Biomater.* **2010**, *6*, 591; c) K. Anselme, *Biomaterials* **2000**, *21*, 667; d) L. C. Xu, C. A. Siedlecki, *Biomaterials* **2007**, *28*, 3273.
[5] J. Rosales-Leal, M. Rodríguez-Valverde, G. Mazzaglia, P. Ramon-Torregrosa, L. Diaz-Rodriguez, O. Garcia-Martinez, M. Vallecillo-Capilla, C. Ruiz, M. Cabrerizo-Vilchez, *Colloids Surf. A* **2010**, *365*, 222.

  

[6] a) M. S. Niepel, D. Peschel, X. Sisquella, J. A. Planell, T. Groth, *Biomaterials* **2009**, *30*, 4939; b) J. Israelachvili, H. Wennerstrom, *Nature* **1996**, *379*, 219.
[7] a) Y. Arima, H. Iwata, *Biomaterials* **2007**, *28*, 3074; b) A. Ranella, M. Barberoglou, S. Bakogianni, C. Fotakis, E. Stratakis, *Acta Biomater.* **2010**, *6*, 2711.
[8] a) S. Faghihi, F. Azari, A. P. Zhilyaev, J. A. Szpunar, H. Vali, M. Tabrizian, *Biomaterials* **2007**, *28*, 3887; b) L. Scheideler, F. Rupp, H. P. Wendel, S. Sathe, J. Geis-Gerstorfer, *Dent. Mater.* **2007**, *23*, 469.
[9] a) S. B. Goodman, Z. Yao, M. Keeney, F. Yang, *Biomaterials* **2013**, *34*, 3174; b) E. B. Hunziker, L. Enggist, A. Kueffer, D. Buser, Y. Liu, *Bone* **2012**, *51*, 98; c) D.-W. Lee, Y.-P. Yun, K. Park, S. E. Kim, *Bone* **2012**, *50*, 974.
[10] J. Zhang, X. Zhu, *Sci. China Chem.* **2009**, *52*, 849.
[11] a) E. Stavrinidou, P. Leleux, H. Rajaona, D. Khodagholy, J. Rivnay, M. Lindau, S. Sanaur, G. G. Malliaras, *Adv. Mater.* **2013**, *25*, 4488; b) J. Liao, S. Wu, Z. Yin, S. Huang, C. Ning, G. Tan, P. K. Chu, *ACS Appl. Mater. Interfaces* **2014**, *6*, 10946.
[12] a) N. K. Guimard, N. Gomez, C. E. Schmidt, *Prog. Polym. Sci.* **2007**, *32*, 876; b) J. Liao, H. Pan, C. Ning, G. Tan, Z. Zhou, J. Chen, S. Huang, *Macromol. Rapid Commun.* **2014**, *35*, 574; c) M. R. Abidian, K. A. Ludwig, T. C. Marzullo, D. C. Martin, D. R. Kipke, *Adv. Mater.* **2009**, *21*, 3764; d) T. Darmanin, F. Guittard, *ChemPhysChem* **2013**, *14*, 2529.
[13] a) L. Xu, Z. Chen, W. Chen, A. Mulchandani, Y. Yan, *Macromol. Rapid Commun.* **2008**, *29*, 832; b) B. Xin, J. Hao, *Chem. Soc. Rev.* **2010**, *39*, 769; c) T. Darmanin, E. T. d. Givenchy, S. Amigoni, F. Guittard, *Adv. Mater.* **2013**, *25*, 1378; d) Y. Zhu, L. Feng, F. Xia, J. Zhai, M. Wan, L. Jiang, *Macromol. Rapid Commun.* **2007**, *28*, 1135; e) J. Isaksson, C. Tengstedt, M. Fahlman, N. Robinson, M. Berggren, *Adv. Mater.* **2004**, *16*, 316.
[14] a) R. B. Pernites, R. R. Ponnapati, R. C. Advincula, *Adv. Mater.* **2011**, *23*, 3207; b) F. Xiao, T. R. Halbach, M. F. Simcik, J. S. Gulliver, *Water Res.* **2012**, *46*, 3101.
[15] J. Liao, C. Ning, Z. Yin, G. Tan, S. Huang, Z. Zhou, J. Chen, H. Pan, *ChemPhysChem* **2013**, *14*, 3891.
[16] a) S. Mukhopadhyay, U. Maitra, *Curr. Sci.* **2004**, *87*, 1666; b) X.-X. Zhu, M. Nichifor, *Acc. Chem. Res.* **2002**, *35*, 539.
[17] D. L. Sampson, Y. L. Chng, Z. Upton, C. P. Hurst, A. W. Parker, T. J. Parker, *Anal. Biochem.* **2013**, *442*, 110.
[18] C. R. Wittmer, J. A. Phelps, W. M. Saltzman, P. R. Van Tassel, *Biomaterials* **2007**, *28*, 851.
[19] D. Khang, J. Choi, Y. M. Im, Y. J. Kim, J. H. Jang, S. S. Kang, T. H. Nam, J. Song, J. W. Park, *Biomaterials* **2012**, *33*, 5997.

  